International Journal of Nanoelectronics and Materials
Volume 13 (Special Issue) Dec 2020 (267-274)

Structural, Microstructure, Dielectric and Magnetic Behavior of Ga Substituted $BiFeO_3$

N. Z. S Noreainia[1], O. H Hassan[2,3], A. M. M Ali[1,2], M. K Yaakob[1], M. Z. A Yahya[4], M. F. M Taib[1*]

[1]*Faculty of Applied Sciences, Universiti Teknologi MARA, 40450 Shah Alam, Selangor, Malaysia.*
[2]*Ionics Materials & Devices (iMADE) Research Laboratory, Institute of Science, Universiti Teknologi MARA, 40450 Shah Alam, Selangor, Malaysia.*
[3]*Faculty of Art and Design, Universiti Teknologi MARA, 40450 Shah Alam, Selangor, Malaysia.*
[4]*Faculty of Defence Science and Technology, Universiti Pertahanan Nasional Malaysia, 57000 Kuala Lumpur, Malaysia.*

ABSTRACT

Galium doped at Bi-site of $Bi_{1-x}Ga_xFeO_3$ (BGFO) ceramics with x = 0.00, 0.01, 0.02 and 0.03 was synthesized by the solid state reaction route. The effect of gallium on structural, microstructure, dielectric and magnetic properties have been investigated. Phases of BGFO were investigated via X-ray Diffractometer has confirmed the formation of a single phase of BGFO where $x \leq 0.02$ is the solid solution limit of gallium. The grain size of BGFO is reduced with the increasing of the Ga concentration. Meanwhile dielectric measurements were performed by using Electrical Impedance Spectroscopy (EIS) at room temperature indicates the inversely proportional pattern for both dielectric constant and dissipation factor in frequency range up to 1MHz. Moreover, substitution in BFO showed a significant improvement in dielectric loss with increasing of Ga content. The magnetic measurement revealed an increase in Ga-content up to 0.02 at room temperature in BGFO can significantly induce the spontaneous magnetization and weak ferromagnetic behavior due to the collapse of spin cycloid structure and modification of antiparallel spin.

Keywords: Bismuth Ferrite, Dielectric, Magnetization.

1. INTRODUCTION

A considerable attention has been drawn to multiferroic class of materials since they are one of the primary targets to researchers either theoretically or experimentally. This is due to their unique and fascinating characteristics which display ferroelectric, ferromagnetic and/or ferroelastic behavior which simultaneously occurred within the same phase in a certain temperature range [1-2]. In search of capable materials for applications, it is essential to have a variety of properties within one material which might be suitable to alter specific device uses [3]. Therefore, multiferroic materials are beneficial in the fundamental view of physics and also play an outstanding role in broad and potential applications of multifunctional devices such as data storages, sensors and spintronics [4]. Perovskite bismuth ferrite, $BiFeO_3$ is acknowledged as a unique and rare material among its kind due to the only known multiferroic materials at room temperature besides $BiMnO_3$ that exhibit ferroelectric properties with high Curie temperature (Tc ~ 1103 K) and show G-type antiferromagnetism properties below Neel temperature (TN ~ 643K) [5] above room temperature. BFO also possesses rhombohedral distorted crystal structure which belongs to the $R3c$ space group [1–3]. BFO which have been discovered in 1960 displays an antiparallel spins arrangement that results in cancellation of any noticeable magnetization and exhibiting loosy type of hysteresis loop that indicates high leakage current as well as high tangent loss which limits their practical applications [6].

*Corresponding Author: *oskar@uitm.edu.my*

The cancellation of net magnetization is attributed by antiferrogmetic spin structure being altered by cycloidal spiral modulated spin structure with spin periodicity of 62 nm which resulted in non-observable macroscopic magnetization [4-6]. Large leakage and low electrical resistivity problems are mainly caused by oxygen vacancies and difficulty in obtaining single phase BFO due to bismuth volatilization during high sintering process that result an impurities appearance such as $Bi_2Fe_4O_9$, $Bi_{36}Fe_{24}O_{57}$ and $Bi_{25}FeO40$. Thus, most of the attention was more focused on the improvement in electrical and destroying cycloid spin structure such as modification of synthesizing methods, doping mechanism and selection of appropriate substitution element [6].

Recently, more works in overcoming this issue was reported. Replacing Bismuth site and Ferrite site with divalents alkaline earth metal (Sr, Ba and Ca) [7–9] and trivalents rare earth metal (Nd, La, Eu, Ho, Sm, Gd, Yb and Y) [10–16] and other compound addition such as $PbTiO_3$ [17] and $BaTiO_3$ [18] show successful enhancement in inducing magnetization and electrical properties. Moreover, various methods of synthesizing have been applied in order to overcome its disadvantages in high volatization of Bismuth ion. The methods stabilize the ion within narrow temperature range and reduce the creation of oxygen vacancies issues in Bismuth Ferrite such as sol gel [19], rapid liquid sintering [20], hydrothermal [21], Pechini method [11] and others. The selection of optimal temperature and substitution of suitable dopant should overcome the volatization issues by suppression of secondary phases which leads to the large leakage current and poor magnetic properties [8]. Most of the researchers had successfully modified BFO using doping or substitution method with appropriate element at Bi-site which leads to stabilization of perovskite structure and control of the appearance of impurities as well enhancement in magnetic properties. In addition, ionic radius of elements does influence the properties of BFO since numerous studies show that by different size of elements could shrink the lattice structure which affect the properties as for instance Sm-doped does show the compression stress generated from smaller ionic substitution with respect to the Bi site [22]. Sm^{3+} substitution also had proven in suppressing the impurities compared to un-doped ones. (Rare earth Eu^{3+} which is smaller in ionic radius compared to Bi^{3+}), was substituted at A-site of BFO system. This suppressed review the spin modulation structure which enhance the magnetization and reduce the presence of impurities [23]. An increasing pattern of dielectric properties with respect to the increase in amount of La dopant which possess larger atomic radius (1.95 Å) compared to Bi [21]. One of the practical ways to improve ferromagnetic properties of BFO is by altering and interrupting antiferromagnetic structure of modulated spin cycloid which holds the locked magnetization [24]. XRD results revealed by La^{3+} doped BFO average crystallite size of nanoparticles declines as the La content increases. The reduction in lattice parameters and volume of unit cell system has also been observed which is caused by smaller ionic radii substitution with respect to Bi^{3+}. The structural transformation of BFO from rhombohedral to orthorhombic as La^{3+} is being introduced and destroyed spin cycloid structure which in turn favor released latent magnetization locked within cycloid structure [25].

In this work, it is proposed that the preparation of Ga^{3+} with smaller ionic radius into A-site of bismuth ferrite $Bi_{1-x}Ga_xFeO_3$ (x = 0.00, 0.01, 0.02 and 0.03) and systematically investigate their structural, microstructure, dielectric and magnetic properties using solid state synthesis route through optimum sintering condition to understand substitution limit that modify the properties of BFO. It is believed this present work is the first time to report the behavior of dielectric and magnetism of $Bi_{1-x}Ga_xFeO_3$.

2. MATERIAL AND METHODS

$Bi_{1-x}Ga_xFeO_3$ or BGFO (x = 0.00, 0.01, 0.02 and 0.03) powders were prepared using solid state method. Highly pure (99.99%) of Bismuth (III) Oxide Bi_2O_3, Iron (III) Oxide Fe_2O_3 and Gallium (III) Oxide Ga_2O_3 powders were appropriately weighed according to the stoichiometric compositions and were mixed together sufficiently. The mixture were grounded using agate

mortar for 2 hours in order to get homogenized. The calcination *temperature was optimized at 800* °C for 2 hours and was grounded again for another 2 hours. Cylindrical pellets were prepared at a dimension diameter of 15 *mm and a thickness of* 2 mm by using hydraulic with a pressure of 6000 psi to 7000 psi. The final sintering schedule was carried out in air 10 °C / hour of heating rate and 10 °C / hour of cooling rate at 825 °C *10 hours for x = 0. While for BGFO compositions,* the sintering hours were decreased *to 9, 8, 7* and 6 hours*, respectively. Phases analysis were carried out via* X-ray diffraction (RIGAKU) *with* 2theta range (20 – 60) using CuK_{α} radiation at slow scanning rate of 3°/min. The grain growth and surface morphology of the samples as Ga content being introduced was investigated by Field emission scanning electron microscope (FESEM) with Pt coating for every sample. Dielectric constant and loss measurement in room temperature were characterized by using Electrical Impedance Spectroscopy (EIS). The magnetic properties of all samples at room temperature condition were investigated using Vibrating Sample Magnetometer (VSM).

3. RESULTS AND DISCUSSION

Figure 1 shows $Bi_{1-x}Ga_xFeO$ (x = 0.00, 0.010, 0.020 and 0.030) sintered at different sintering hours 10 hours, 9 hours, 8 hours and 7 hours respectively. No impurities were detected for gallium dopant at Bi site for concentration of x = 0.00, 0.01 and 0.02. All compositions were indexed according to the pure BFO XRD pattern. It is noted that by gallium dopant at certain value of x = 0.00, 0.01 and 0.02 does suppress the Bi loss mechanism during sintering at high temperature where normally $Bi_2Fe_4O_9$ and $Bi_{25}FeO_{39}$ phase does occur during heat treatment process. It also indicates that the gallium substitution suitable for low concentration doping since secondary phases only existed at concentration of x = 0.03.

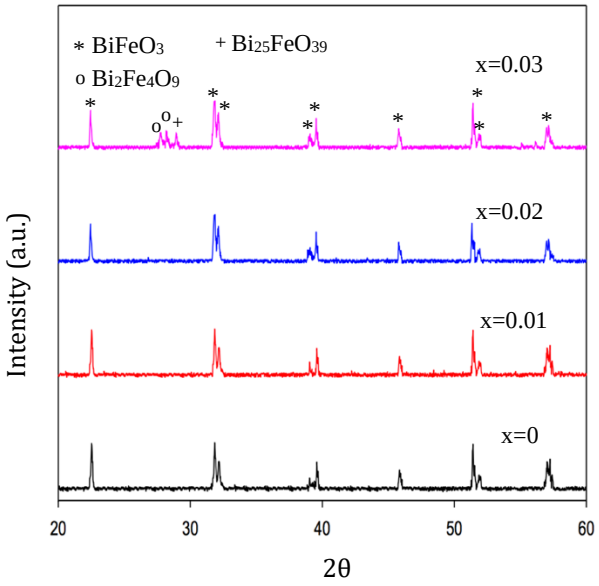

Figure 1. XRD patterns of $Bi_{1-x}Ga_xFeO_3$ (x=0.00, 0.01, 0.02 and 0.03) ranging between $20 \leq 2\theta \leq 60$.

The cell volume of the crystal structure BFO indicated a decreasing pattern shown in Table 1 as Ga^{3+} doping concentration increase by replacing Bi^{3+}. It is observed the structure undergo contraction since the lattice parameters as well as volume of unit cell are decreasing with increasing of Ga^{3+} concentration. The calculated lattice parameter values (a, c) also appeared to have some changes as a result of Ga substitution that may be attributed to the replacing of smaller ionic radius of Ga^{3+} (0.62 Å) compared to Bi^{3+} (1.03 Å) ions consequently change the volume of BFO structure.

Figure 2 shows the FESEM micrograph for $Bi_{1-x}Ga_xFeO_3$ sintered at different temperatures for x = 0.00, 0.010, 0.020 and 0.030. From the micrograph, it can be observed that the dense and well-developed grain were non-uniformly distributed. It can be found that the grain sizes of all samples were significantly decreased with the increasing of Ga^{3+} content and for un-doped sample the grain are more circular.

Table 1 Lattice parameter and volume of $Bi_{1-x}Ga_xFeO_3$

Composition (x)	a (Å)	c (Å)	Volume (Å)^3
0.00	5.5810	13.8760	374.30
0.01	5.5788	13.8570	373.50
0.02	5.5760	13.7540	370.34
0.03	5.5690	13.7400	369.03

As the gallium concentration increased (x = 0.00, 0.01, 0.02 and 0.03), the grains became more angular in shape and more uniformed due to the introduction of smaller ionic radius of Ga^{3+} to the Bi-site which aligned with the compression of BGFO volume of structure shown in lattice parameters calculation.

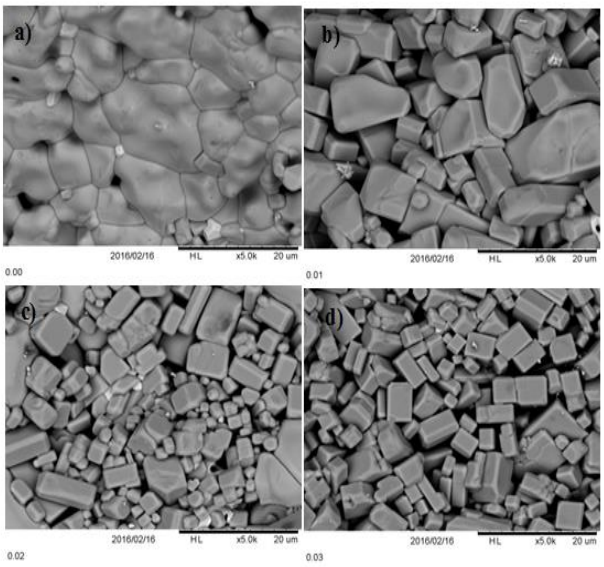

Figure 2. SEM images of $Bi_{1-x}Ga_xFeO_3$ for composition (a) x=0.00 (b) x=0.01 (c) x=0.02 and (d) x=0.03.

Figures 3a and 3b show the dielectric constant and dielectric loss as function of frequency for $Bi_{1-x}Ga_xFeO_3$ (x = 0.00, 0.010, 0.020 and 0.030) samples that were carried out at room temperature. Ga dopant did play an important role in altering the dielectric behavior of BGFO samples where dielectric constant values decreased with respect to the frequency as the concentration of Gallium doping increase. The frequency dependence for both dielectric constant and loss which identical behavior in line with the previous literature [13 - 15]. At low frequencies space charges were unable to follow electric field results in exhibition of high dielectric constants and during high frequency they underwent relaxation which constant patterns were obtained. Meanwhile for dielectric loss, un-doped and BGFO samples exhibit a decrease in loss value as the Ga concentration increased at the Bi site but all samples did not exhibit relatively high dielectric loss values.

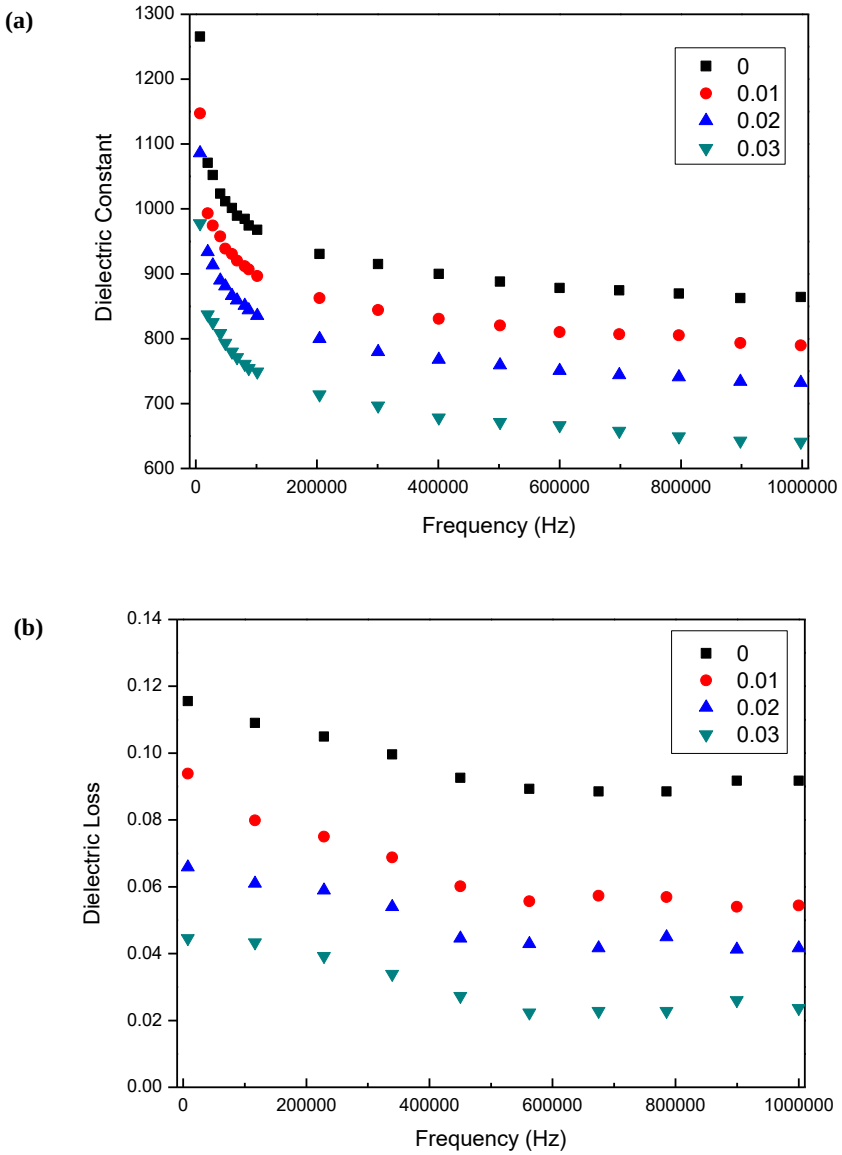

Figure 3. (a) Dielectric constant and (b) Dielectric Loss as a function of frequency for BGFO ceramics.

The decrease of dielectric loss with the increase of Ga^{3+} dopant could be helpful in producing good electrical practical application. Ga^{3+} content of all samples with respect to the dielectric constant is shown in Figure 4. The graph shows the proportional behavior that indicates drastic changes of dielectric constant ranging from undoped to 3% of Ga doping concentration where x = 0.03 does display maximum value of 1290 at room temperature. Figure 4 demonstrated the variation of dielectric loss as a function of Ga content which the enhancement can be seen as Ga^{3+} being introduced in BFO system. While for gallium with concentration 0.03 demonstrated a good dielectric result with high dielectric constant and low dielectric loss.

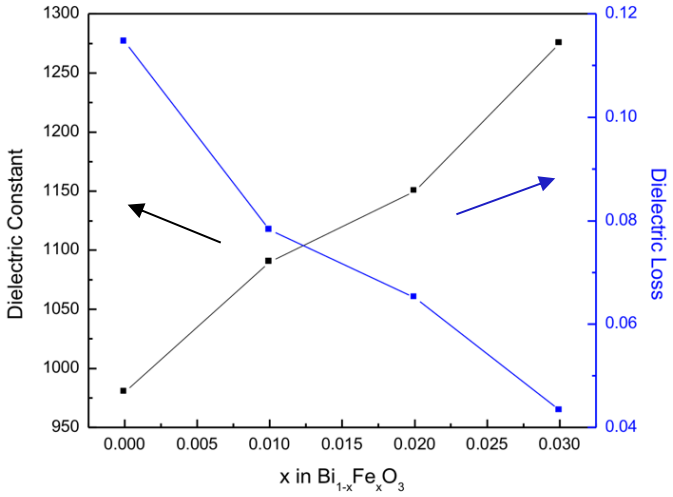

Figure 4. Variation of dielectric constant and dielectric loss with Ga^{3+} content for of $Bi_{1-x}Ga_xFeO$ samples (0.00, 0.01, 0.02 and 0.03).

Figure 5 shows magnetization of all samples as a function of the magnetic applied field for $Bi_{1-x}Ga_xFeO_3$ at room temperature. All samples achieved saturation magnetization at 6K Oe of magnetic field with values range of 0.0081 emu/g - 0.03 emu/g. The linear line exhibited by pure Bismuth indicates the basic antiferromagnetic nature due to the antiparallel spin orientation that limits the production of any magnetization values. Obviously, BFO also exhibited almost no net magnetization and unsaturated hysteresis loop (linear) due to the locked cycloid spin structure which indicates antiferromagnetism dominated in this material. The well-developed magnetic hysteresis loop M-H can be detected in the same magnetic field. As expected, the Ga^{3+} doping samples exhibited a non-linear magnetization, with nonzero remnant magnetization (Mr) and coercive field (Hc) for all doped samples which indicate an appearance of ordered magnetic structure. It can be seen that hysteresis loop features were exhibited by concentration up until x = 0.02 at Bi-site of BFO. At 0.01 and 0.02 compositions enhancement in magnetization value might be due to the destroyed cycloid spin structure since the introduction of Ga^{3+} dopant that caused lattice distortion which would affect the increments of magnetization value. At 3% of Gallium substitution to BFO system shows a decrease in magnetization due to secondary phases such as $Bi_2Fe_4O_9$ and $Bi_{25}FeO_{39}$ can be detected which most of the impurities exhibit non-magnetic behavior consequently lowering the magnetization values.

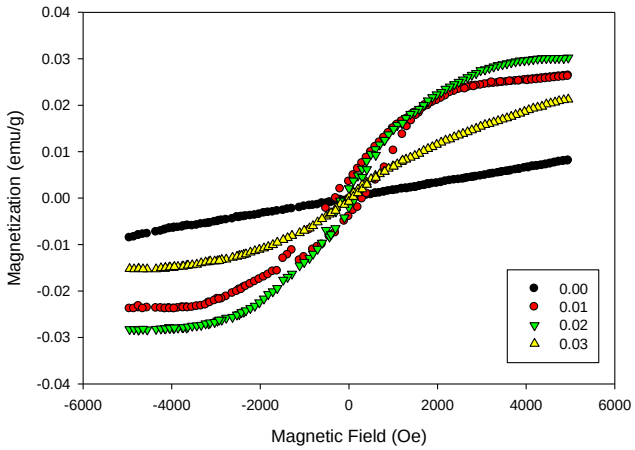

Figure 5. Variation of magnetization with Ga content for of $Bi_{1-x}Ga_xFeO_3$ samples (x=0.00, 0.01, 0.02 and 0.03).

4. CONCLUSION

The $Bi_{1-x}Ga_xFeO_3$ (x = 0.00, 0.010, 0.020 and 0.030) compounds were successfully prepared using solid state synthesis route. The formation of single phase of BFO was obtained for $x \leq 0.02$. The effect of Ga substitution on BFO grains is denser with uniform size. This lead to high dielectric constant and smaller loss compared to pure BFO. The magnetic measurement by VSM revealed the enhancement in magnetization value with respect to the un-doped BFO. Overall, the properties of BGFO are closely related with the ionic radius and depending on the sizes and amount of dopant. Thus, substitution of smaller ionic radius to the A-site of $BiFeO_3$ is evidently to be useful in tailoring structural and dielectric and magnetic properties.

ACKNOWLEDGEMENTS

This work was supported by Ministry of Higher Education (MOHE) Malaysia under FRGS grant 600-IRMI/FRGS 5/3 (337/2019) and University Technology MARA (UiTM) for the facilities provided.

REFERENCES

[1] Shami, M. Y., Awan, M. S., & Anis-ur-Rehman, M., Key Eng. Mater. **510–511** (2012) 348–355.
[2] Guo, H. F., Guo, S. X., & Ben Li, L., Appl. Mech. Mater. **164** (2012) 115–119.
[3] Gotardo, R. A. M., Montanher, D., Protzek, O. A., Cótica, L.F., Santos, I. A., Viana, D. S. F., Nascimento, W. J., Garcia, D., & Eiras, J. A., Adv. Mater. Res. **975** (2014) 257–262.
[4] Uchida, H., Nakaki, H., Funakubo, H., Koda, S., Key Eng. Mater. **320** (2006) 49–52.
[5] Liu, X. L., Dou, X. L., Xie, H. Y., & Chen, J. F., Key Eng. Mater. **512–515** (2012) 1235–1239.
[6] Li, X. A., Li, P., Li, Y. T., Yang, J. P., Bai, Q. F., Liu, Z. R., & Wang, B. L, Key Eng. Mater. **512–515** (2012) 1434–1437.
[7] Thakur, S., Pandey, O. P., & Singh, K., Ceram. Int. **3** (2014) 1–9.
[8] Chaudhuri, A., & Mandal, K., J. Magn. Magn. Mater. **353** (2014) 57–64.
[9] Thakur, S., Pandey, O. P., & Singh, K., J. Mol. Struct. **1074** (2014) 186–192.
[10] Chen, D. G., Tang, X. G., Liu, Q. X., Cheng, X. F. & Zou, Y., Mater. Sci. Forum **687** (2011) 439–446.
[11] García-Zaleta, D. S., Torres-Huerta, A. M., Domínguez-Crespo, M. A., Matutes-Aquino, J. A., González, A. M., & Villafuerte-Castrejón, M. E., Ceram. Int. **40**, **7** (2014) 9225–9233.
[12] Basu, A., & Mukherjee, G. D., Solid State Commun. **189** (2014) 5–9.
[13] Pradhan, S. K., Das, J., Rout, P. P., Mohanta, V. R., Das, S. K., Samantray, S., Sahu, D. R., Huang, J. L., Verma, S., & Roul, B. K., J. Phys. Chem. Solids **71** (2010) 1557–1564.
[14] Ain, R. S. N., Halim, S. A., & Hashim, M., Adv. Mater. Res. **501** (2012) 329–333.
[15] Song, G. L., Wang, T. X., Xia, C. J., Li, C., & Chang, F. G., Adv. Mater. Res. **150–151**, 1470–1475.
[16] Medina, L. M. S., Jorge, G. A., & Martín Negri, R., J. Alloys Compd. **592** (2014) 306–312.
[17] Esat, F., Comyn, T. P., & Bell, A. J., Acta Mater. **66** (2014) 44–53.
[18] Gupta, R., Shah, J., Chaudhary, S., & Kotnala, R. K., J. Alloys Compd. **638** (2015) 115–120.
[19] Du, Y., Cai, K. F., Li, H., & An, B. J., J. Electron. Mater. **40** (2011) 518–522.
[20] H. Dai, Z. Chen, R. Xue, T. Li, J. Chen, & H. Xiang, "Structural and electric properties of polycrystalline Bi1−xErxFeO3 ceramics," Ceram. Int. **39**, 5 (2013) 5373–5378.
[21] Chaudhuri, A., & Mandal, K., Mater. Res. Bull. **47** (2012) 1057–1061.
[22] Dai, H., Chen, Z., Li, T., & Li, Y., J. Rare Earths **30** (2012) 1123–1128.
[23] Chandra, P., Kumar, M., Chhoker, S., & Jewariya, M., Ceram. Int. **41** (2015) 2389–2398.
[24] Pradhan, S. K., Das, J., Rout, P. P., Das, S. K., Mishra, D. K., Sahu, D. R., Pradhan, A. K., Srinivasu, V. V., Nayak, B. B., Verma, S., & Roul, B. K., J. Magn. Magn. Mater. **322** (2010) 3614–3622.
[25] Basiri, M. H., Shokrollahi, H., & Isapour, G., J. Magn. Magn. Mater. **354** (2014) 184–189.